PACS: 81.05.Zx

Effect of the hatching strategies on mechanical properties and microstructure of SEBM manufactured Ti-6Al-4V specimens

(Supplementary material)

Popov Jr. Vladimir V. †[1], Alexander Katz-Demyanetz1, Kovalevsky Aleksey [1], Biletskiy Roman [1], Strokin Evgeny [1], Garkun Andrey [1], Bamberger Menachem [2]
† vvp@technion.ac.il

[1] Israel Institute of Metals, Technion R&D Foundation, Technion City, Haifa 3200003, Israel
[2] Department of Materials Science and Engineering, Technion – Israel Institute of Technology, Technion City, Haifa 3200003, Israel

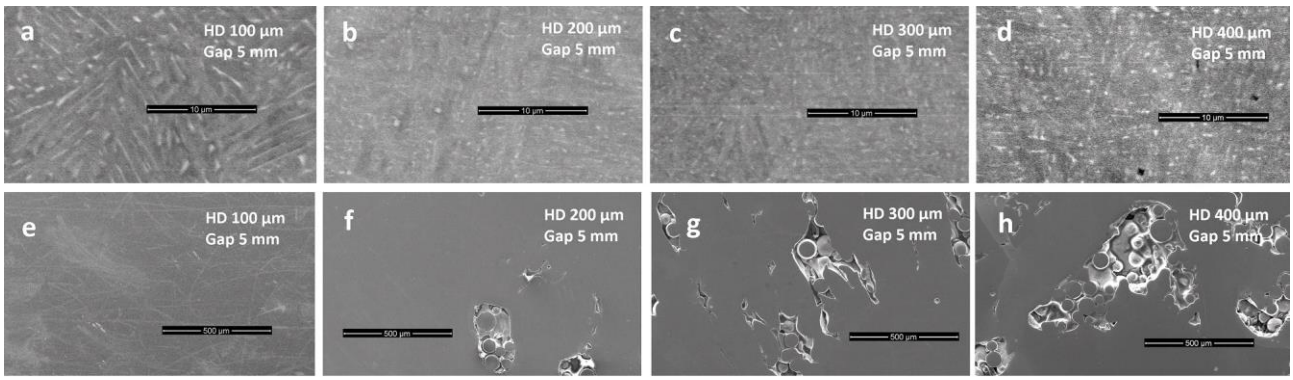

Fig. S1. Ti-6Al-4V SEBM manufactured samples from set №2 (gap 5 mm). Backscattered electron images of the microstructure with: HD=100 µm (a); HD=200 µm (b); HD=300 µm (c); HD=400 µm (d). SEM-images of defects propagation: HD=100 µm (e); HD=200 µm (f); HD=300 µm (g); HD=400 µm (h).

Table S1. Tensile properties of the samples printed at various distances through increase of hatching distance

Distance between printing during, mm	HD, µm	Tensile strength, MPa	Yield strength MPa	Cross-sectional area reduction, %	Elongation at fracture, %
10	100	1034.0±4.4	967.0±0.0	42.3±6.5	18.3±0.7
	200	1022.0±8.5	958.5±4.9	0.0±0.0	2.3±0.4
	300	455.3±9.1	424.7±11.1	0.0±0.0	0.0±0.0
	400	187.0±38.2	173.0±28.3	0.0±0.0	0.0±0.0
5	100	1033.7±2.9	962.7±5.5	43.4±6.2	18.7±0.5
	200	1008.3±5.7	957.3±5.5	0.0±0.0	3.4±0.5
	300	411.7±25.1	398.0±23.1	0.0±0.0	0.0±0.0
	400	206.0±2.8	184.5±0.7	0.0±0.0	0.0±0.0
2	100	1043.7±8.4	983.0±8.2	42.4±0.6	17.7±0.2
	200	1007.7±4.9	930.7±6.7	41.7±6.3	18.8±0.5
	300	884.0±6.6	830.7±8.6	0.0±0.0	0.8±0.1
	400	454.5±57.3	435.5±30.4	0.0±0.0	0.0±0.0

Table S2. Tensile properties of the samples printed at various distances through decrease of hatching distance

Distance between printing during, mm	HD, µm	Tensile strength, MPa	Yield strength MPa	Cross-sectional area reduction, %	Elongation at fracture, %
10	100	1146.0±5.7	1079.0±7.1	8.0±0.0	5.5±1.6
	80	1083.5±9.2	1159.5±4.9	11.0±0.0	7.6±0.3
	50	994.0±52.3	996.5±51.6	0.0±0.0	0.0±0.0

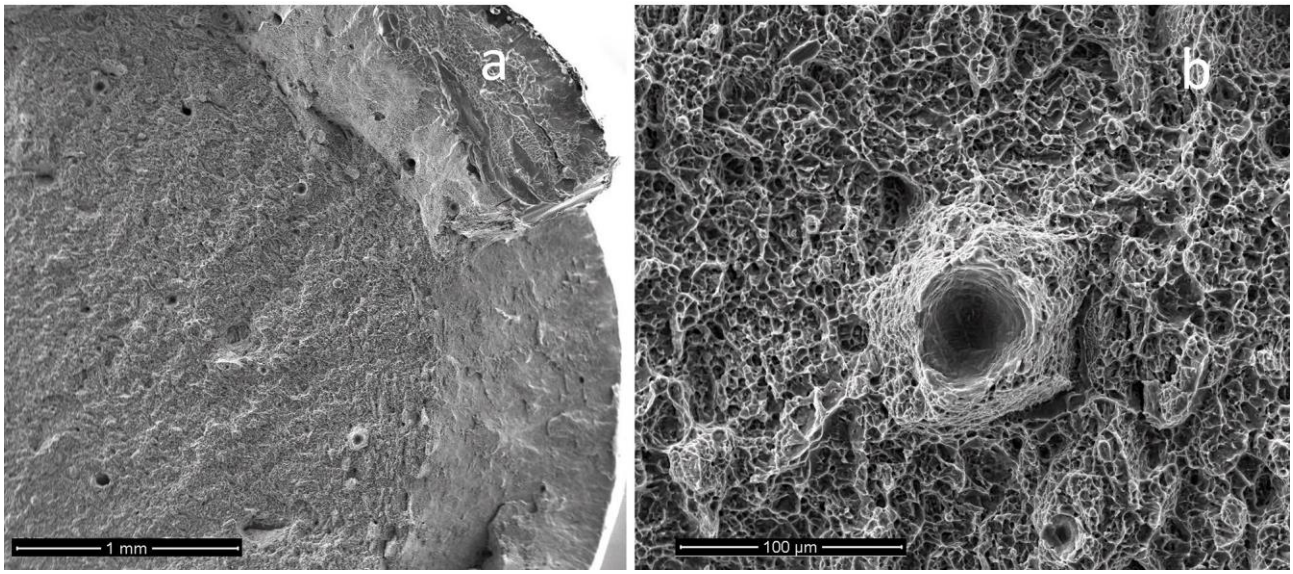

Fig. S2. SEM-images on the fractured surface: with low (x 100, a); and high (x 1500, b) magnification. Set №1: gap 10 mm, HD 100 µm.

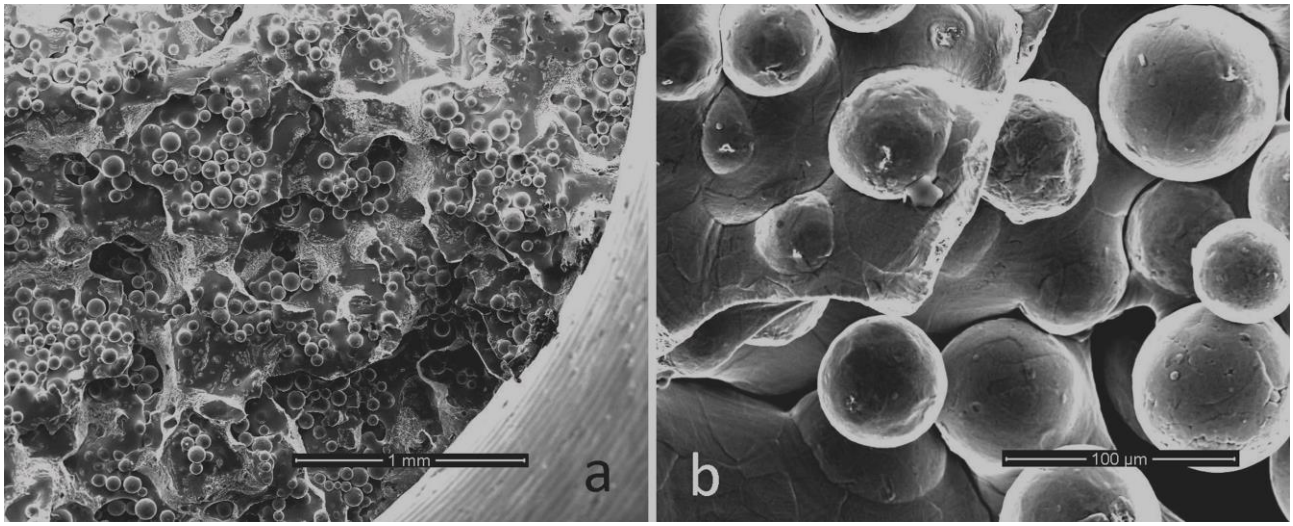

Fig. S3. SEM-images on the fractured surface: with low (x 100, a); and high (x 1500, b) magnification. Set №1: gap 10 mm, HD 300 µm.

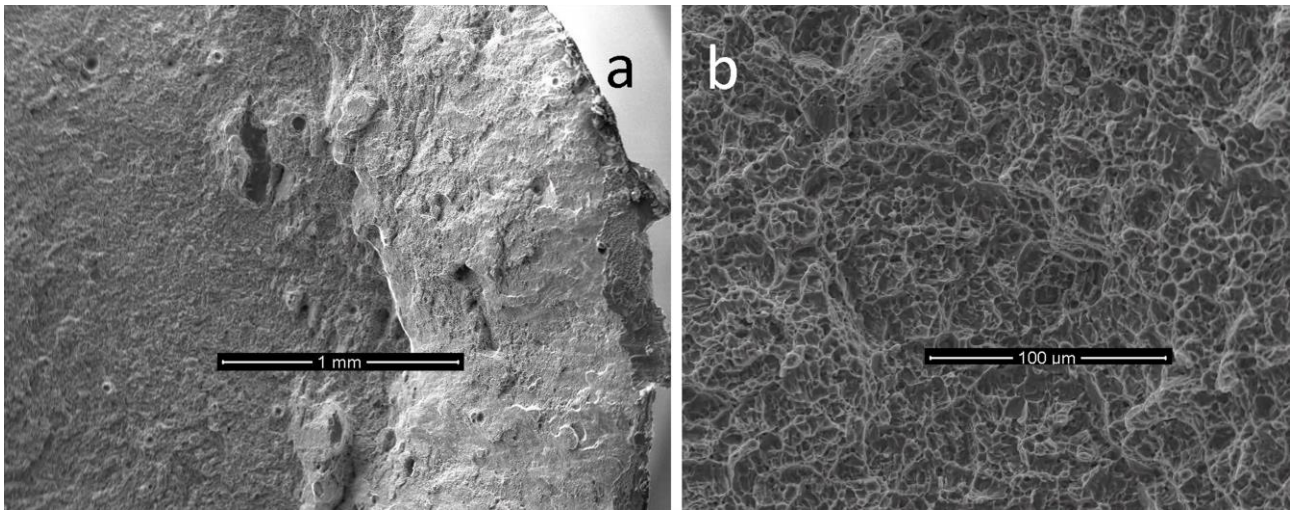

Fig. S4. SEM-images on the fractured surface: with low (x 100, a); and high (x 1500, b) magnification. Set №2: gap 5 mm, HD 100 µm.

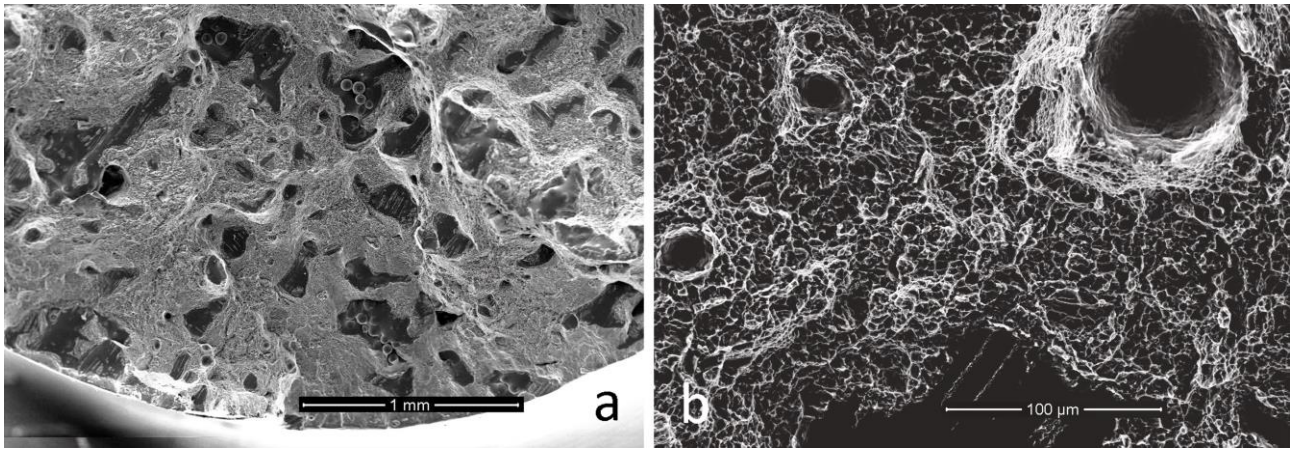

Fig. S5. SEM-images on the fractured surface: with low (x 100, a); and high (x 1500, b) magnification. Set №2: gap 5 mm, HD 200 µm.

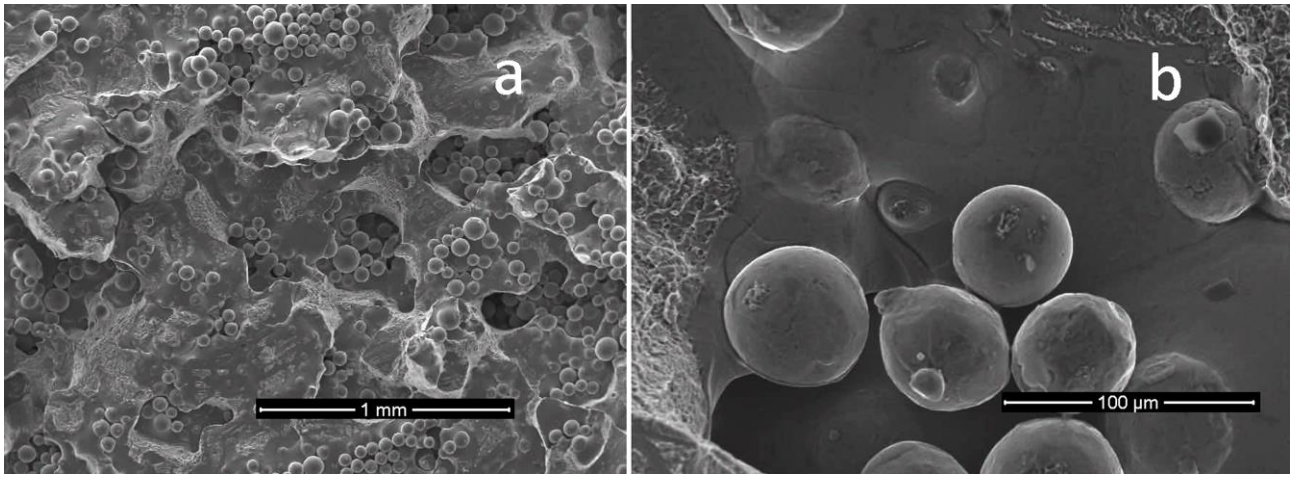

Fig. S6. SEM-images on the fractured surface: with low (x 100, a); and high (x 1500, b) magnification. Set №2: gap 5 mm, HD 300 µm.

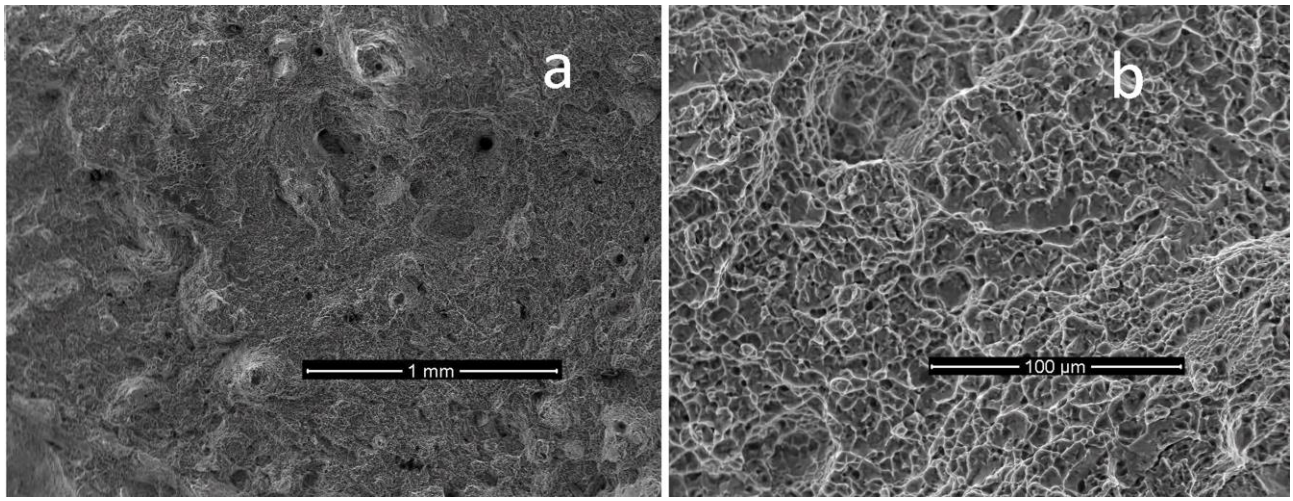

Fig. S7. SEM-images on the fractured surface: with low (x 100, a); and high (x 1500, b) magnification. Set №3: gap 2 mm, HD 100 µm.

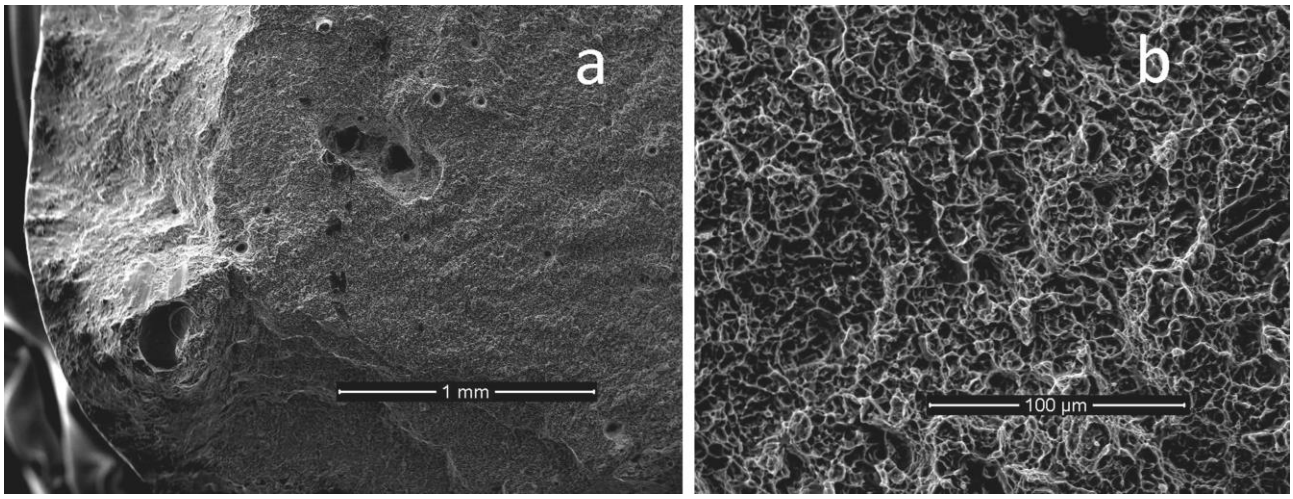

Fig. S8. SEM-images on the fractured surface: with low (x 100, a); and high (x 1500, b) magnification. Set №3: gap 2 mm, HD 200 µm.

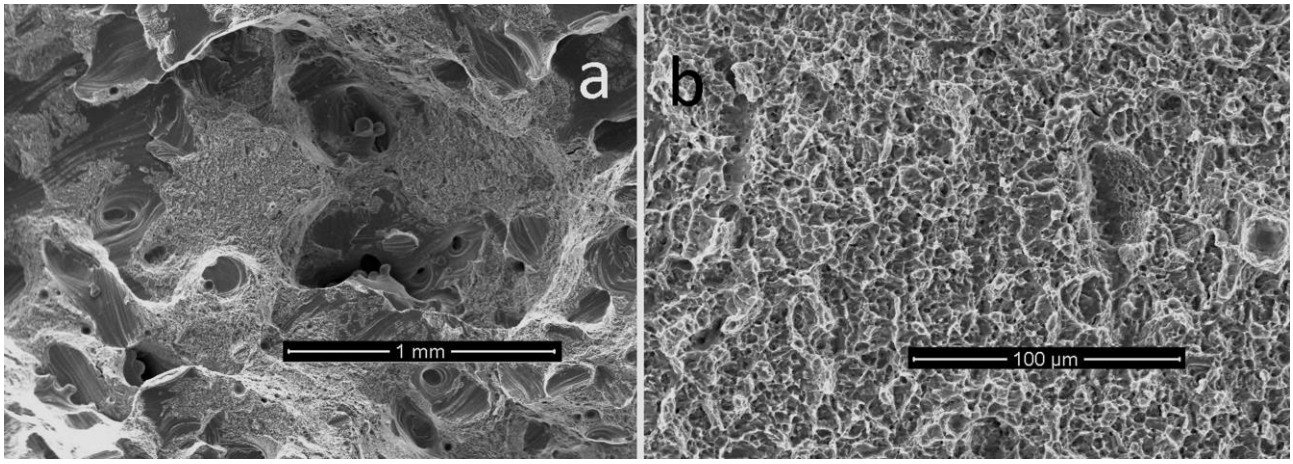

Fig. S9. SEM-images on the fractured surface: with low (x 100, a); and high (x 1500, b) magnification. Set №3: gap 2 mm, HD 300 µm.